Assessing the impact of distortion correction on Gamma Knife radiosurgery for multiple metastasis: Volumetric and dosimetric analysis

Yavuz Samanci [a,b], M. Orbay Askeroglu [b], Ali Haluk Düzkalir [b,c], Selcuk Peker [a,b,*]

[a] Department of Neurosurgery, Koc University School of Medicine, Istanbul, Turkey
[b] Gamma Knife Center, Department of Neurosurgery, Koc University Hospital, Istanbul, Turkey
[c] Department of Neurosurgery, Koc University Hospital, Istanbul, Turkey

ABSTRACT

Introduction: Magnetic resonance imaging (MRI) is a robust neuroimaging technique and is the preferred method for stereotactic radiosurgery (SRS) planning. However, MRI data always contain distortions caused by hardware and patient factors.
Research question: Can these distortions potentially compromise the effectiveness and safety of SRS treatments?
Material and methods: Twenty-six MR datasets with multiple metastatic brain tumors (METs) used for Gamma Knife radiosurgery (GKRS) were retrospectively evaluated. A commercially available software was used for distortion correction. Geometrical agreement between corrected and uncorrected tumor volumes was evaluated using MacDonald criteria, Euclidian distance, and Dice similarity coefficient (DSC). SRS plans were generated using uncorrected tumor volumes, which were assessed to determine their coverage of the corrected tumor volumes.
Results: The median target volume was 0.38 cm^3 (range,0.01–12.38 cm3). A maximum displacement of METs of up to 2.87 mm and a median displacement of 0.55 mm (range,0.1–2.87 mm) were noted. The median DSC between uncorrected and corrected MRI was 0.92, and the most concerning case had a DSC of 0.46. Although all plans met the optimization criterion of at least 98% of the uncorrected tumor volume (median 99.55%, range 98.1–100%) receiving at least 100% of the prescription dose, the percent of the corrected tumor volume receiving the total prescription dose was a median of 95.45% (range,23.1–99.5%).
Discussion and conclusion: MRI distortion, though visually subtle, has significant implications for SRS planning. Regular utilization of corrected MRI is recommended for SRS planning as distortion is sometimes enough to cause a volumetric miss of SRS targets.

1. Introduction

Metastatic brain tumors (METs) occur in 20–40% of cancer patients, and stereotactic radiosurgery (SRS) is a valuable option for their management. SRS provides precise and non-invasive radiation delivery to target lesions with the help of advanced imaging techniques, particularly MRI, which is known for its soft tissue contrast and anatomical visualization (Niranjan et al., 2019; Putz et al., 2020; Vogelbaum et al., 2022). However, the presence of distortions within MRI data poses a significant challenge, potentially compromising SRS accuracy and safety

with target underdosing (29–53%) and/or radiation-induced toxicity (Lightstone et al., 2005; Seibert et al., 2016; Pappas et al., 2017; Jacobson et al., 2021). Although up to 2.6 mm distortions can be observed with MRI (Wang et al., 2013; Weygand et al., 2016) and inaccuracies as small as 1 mm can lead to considerable changes in the dosimetric properties of the treatment plan (Karaiskos et al., 2014), unfortunately, distortion correction is not consistently implemented in clinical practice, possibly due to a lack of awareness or perceived insignificance of these effects (Baldwin et al., 2007).

The Leksell Gamma Knife® (LGK) is a dedicated platform for

intracranial SRS, and research shows its increasing success in treating METs with Gamma Knife radiosurgery (GKRS) (Bowden et al., 2019; Benjamin et al., 2021; Yamamoto et al., 2021; Wei et al., 2022). Given the higher conformity and steep dose gradients in GKRS plans, there is a need for improved spatial accuracy. It is worth noting that even subtle distortions on modern scanners, though visually undetectable, can greatly affect the precision and accuracy of GKRS, especially in small lesions (Karaiskos et al., 2014). MRI distortions can not only affect the accuracy of identifying and outlining targets and critical organs but also impact the precision of co-registration MRI images with CT scans, a common procedure in SRS (Brock et al., 2017). Reducing distortion levels is thus essential to ensuring treatment effectiveness is not jeopardized. This can be achieved through built-in methods provided by MRI manufacturers or through various post-processing techniques aimed at distortion correction, primarily utilizing reversed read gradient or field mapping methods (Chang and Fitzpatrick, 1992; Jezzard and Balaban, 1995; Morgan et al., 2004). Although correction programs provided by manufacturers are designed to mitigate distortions, they might not fully eliminate them (Wang et al., 2004; Walker et al., 2014).

This article aims to explore the effect of distortion in GKRS and highlight the importance of distortion correction for multiple METs.

2. Material and methods

2.1. Study design and population

We conducted a retrospective analysis of MR datasets to assess the potential impact of distortion. All 26 participants in this study underwent single fraction GKRS for multiple METs (70 METs). The patients had a median age of 60 years (range 41–84 years), with 58% of them being female. The Institutional Review Board of Koç University approved this retrospective study (2022.021.IRB1.058016). Patient consent was waived as only fully anonymized images were used.

2.2. Imaging, distortion correction, tumor delineation, and Preplan measurements

Preplanning reference computed tomography (CT) scans were acquired with a Siemens SOMATOM Definition AS CT scanner (Siemens Medical Solutions, Erlangen, Germany) (100 kV, 352 mAs, 4-mm slice thickness, 250-mm field of view, 512 × 512 matrix, and 1 mm reconstructed in-plane resolution). After that, 3D T1-weighted, post-gadolinium images were acquired with three different Siemens MR scanners (Siemens Medical Solutions, Erlangen, Germany) according to the GKRS protocol for brain metastases: Siemens MAGNETOM Espree 1.5T (TE 3.31 ms, TR 6.2 ms, flip angle 10°, 320 × 320 matrix), Siemens MAGNETOM Aera 1.5T (TE 4.77 ms, TR 7.83 ms, flip angle 12°, 320 × 320 matrix) and Siemens MAGNETOM Skyra 3.0T (TE 3.04 ms, TR 8.07 ms, flip angle 12°, 256 × 256 matrix). During the MR imaging, no stereotactic frame, localization box, or any other apparatus was used. This was possible because the LGK Icon™ incorporates an integrated stereotactic cone-beam CT (CBCT) system, allowing avoidance of frame-induced distortions or susceptibility-related artifacts (Pappas et al., 2016).

The CT and MR datasets were co-registered using Elements Image Fusion (release 4.0.2.8), and the Distortion Correction application (release 4.0.2.8) was used to correct MR distortion. The Elements Cranial Distortion Correction application is designed to correct distortions in MR images and is already implemented in the Brainlab Elements software suite (Brainlab AG, Munich, Germany) (Hiepe, 2017). This technique does not need prior information on MRI acquisition. Before applying the algorithm, it is necessary to perform a rigid registration of CT and MR datasets. This method is unsuitable for MR-only or synthetic CT workflows. The algorithm aligns MRI images to a geometrically accurate, distortion-free planning CT through multiple rigid CT-MR registrations of overlapping subvolumes measuring 3 × 3 × 3 cm³ to address any local mismatches. These localized registrations are

subsequently interpolated to create a continuous 3D deformation field that corrects the fused MR images (Fig. 1). As a result, the algorithm produces a corrected MR dataset that can be utilized for tumor delineation. The algorithm and software have undergone prior validation (Calvo-Ortega et al., 2019; Retif et al., 2022). Following distortion correction, targets were delineated using Elements SmartBrush (release 4.0.0.108), and necessary revisions were made by the senior author. After distortion correction, the manufacturer-specified distortion field was re-applied using in-house software (Brainlab AG, Munich, Germany) for direct comparison between corrected and uncorrected tumor volumes on the same MR image (Fig. 2) (Seibert et al., 2016). This approach avoids additional contouring steps and minimizes measurement variability (Stanley et al., 2013).

The Euclidean distance (3D) between the center of mass of the uncorrected and corrected tumor volumes was quantified for each lesion in millimeters. This measurement allows for assessing the spatial discrepancy between the center of mass positions before and after applying the distortion correction. The Macdonald criteria (Macdonald et al., 1990), which involves measuring the longest diameter (Ld) across all slices and the longest perpendicular diameter (LPd) within the slice where the longest diameter is identified, were calculated for each target. Pass/fail values for the Macdonald criteria and Euclidean distance were set at 1 mm, corresponding to the voxel size (Calvo-Ortega et al., 2019). The agreement between uncorrected and corrected targets was evaluated using the Dice similarity coefficient (DSC), which measures the overlap between two delineated structures (Dice, 1945). The DSC value ranges from 0 to 1, with higher values indicating better agreement. A DSC value of 0.41–0.60 was considered poor, 0.61–0.80 as medium, and 0.81–1.00 as satisfactory agreement (Retif et al., 2022).

2.3. Treatment planning and distortion measurement

The structure and MR datasets were exported to Leksell Gamma Plan® Lightning (version 11.3.2). An automated SRS plan was created using each uncorrected tumor volume to evaluate the clinical impact of anatomic distortion. These plans were then analyzed to assess the coverage of the corrected tumor volume, providing insight into the dose distribution that would be achieved if the distortion had not been corrected. The SRS prescription dose was set at 20 Gy for each lesion, and all comparisons were made based on relative dose measurements. In this analysis, no margin was included as it can vary between institutions and would only amplify the impact of the distortion by increasing the volumes affected. The plan optimization was set to ensure that intended planning goals, such as high-dose conformity and steep dose gradients, were achieved (Samanci et al., 2021). The median number of shots was 6 (range, 1–61), and the prescription isodose was set to cover >98% of each target volume. The corrected tumor volume was considered missed if more than 10% of its volume received less than 90% of the prescription dose (Seibert et al., 2016). Corresponding V_{18}, D_{min}, D_{mean}, and D_{max} values were also determined for all targets.

2.4. Statistical analysis

All statistical analyses were performed using the Statistical Package for Social Sciences 29.0 (SPSS Inc., Chicago, IL, USA). Descriptive statistics, including median, range, mean, and standard deviation, were used to summarize the demographic, radiological, and radiosurgical characteristics of the cohort. The Fisher exact test, t-test, Kaplan-Meier analysis, and Cox regression models were applied as appropriate. Two-sided tests were conducted, and a significance level of $p < 0.05$ was considered statistically significant.

3. Results

A total of 70 METs, located mostly in the frontal lobe (37.1%), were investigated (Table 1). Most of the METs (57.1%) were located
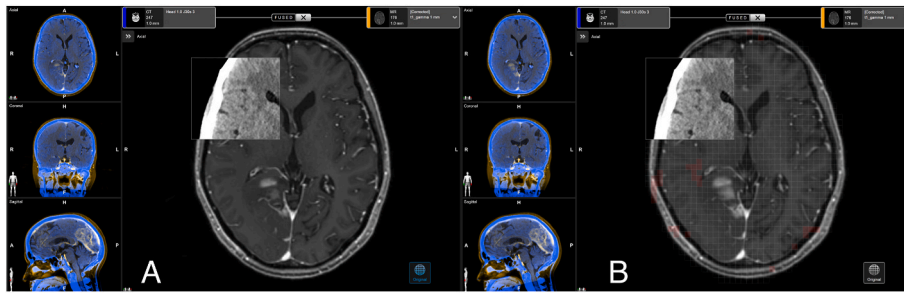
Fig. 1. The Distortion Correction application providing a visual representation of the distortion map (right side) after correcting an MR dataset (left side).
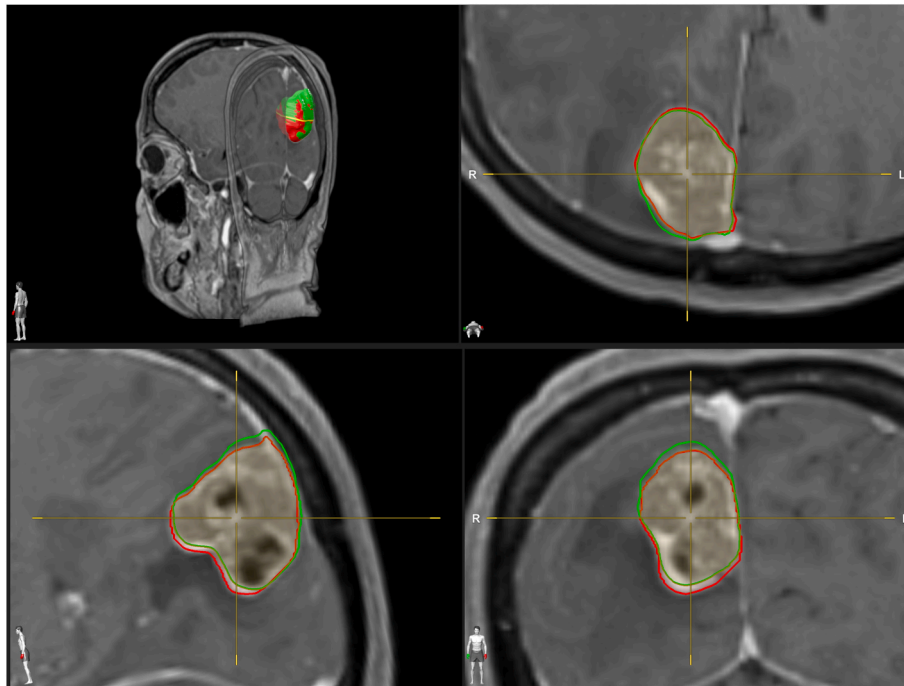

Fig. 2. Figure provides axial, sagittal, and coronal views that depict the original target volume (green contour) and its corresponding corrected target volume (red contour).

peripherally, with a mean isocenter distance of 69.1 ± 7.42 mm, and only three lesions (4.3%) were in the air-bone neighborhood. The median target volume was 0.38 cm^3 (range 0.01–12.38 cm^3). The distortion caused a maximum displacement of up to 2.87 mm, and the median displacement was 0.55 mm. The mean difference between the Ld and the LPd between uncorrected and corrected volumes were 0.3 ± 0.3 mm and 0.5 mm ± 0.48 mm, respectively. Overall, the differences observed in the Macdonald criteria were within the voxel size, with a rate of 97.1% for the Ld and 85.7% for the LPd. Comparing the volumes from uncorrected and corrected MRI, the median DSC was 0.92, and the most concerning case had a DSC of 0.46.

All SRS plans on the uncorrected datasets met the optimization criterion, with at least 98% of the uncorrected tumor volume (median 99.55%, ranging from 98.1% to 100%) receiving at least 100% of the prescribed dose. Following correction, the median coverage was reduced to 95.45% (range 23.1–99.5%). Eighteen (25.7%) retained coverage of 98–100%, and 52 (74.3%) METs did not meet the criterion for adequacy in the SRS plan. Fig. 3 presents a MET where the coverage has undergone a noticeable alteration. The METs that retained coverage had a significantly larger mean volume than METs that showed reduced coverage (4.9 vs. 0.9 cm^3, p < 0.001) (Fig. 4). The METs that exhibited reduced coverage were observed to be positioned at a greater distance from the image isocenter; however, this disparity did not reach

statistical significance (59.9 ± 17.28 vs. 57.7 ± 12.53 mm, p = 0.618). According to the 10% criterion, three of the METs were considered geometric misses, with a mean coverage of 73.8%. Comparing the D_{min}, D_{mean}, and D_{max} values, a statistically significant reduction was found in corrected structures in D_{min} (1.8 Gy (95% CI, 1.2–2.3 Gy), t(69) = 6.404, p < 0.001, d = 0.765) and D_{mean} (0.4 Gy (95% CI, 0.2–0.6 Gy), t(69) = 4.597, p < 0.001, d = 0.549).

4. Discussion

MRI distortion can lead to inaccuracies in the localization of intracranial targets during SRS. Our study reveals that when using uncorrected MRI for target delineation, there can be a deviation of several millimeters in the resulting contours from the actual target position, as observed in previous studies (Moerland et al., 1995; Stanescu et al., 2008; Seibert et al., 2016; Calvo-Ortega et al., 2019; Jacobson et al., 2021; Retif et al., 2022). In the context of precise SRS treatment plans, these millimeter-level displacements can result in significant under-dosing of the actual target. These shifts may go unnoticed without correcting for distortion, and the resulting misalignment could potentially be misinterpreted as treatment failures (Putz et al., 2020).

SRS, which originated from a 1951 publication by Lars Leksell (1951), has evolved with the development of LGK devices for clinical use

Table 1
Demographic, radiological, distortion and Gamma Knife radiosurgery features of the study participants.

Variable	Mean (SD)	n (%)	Range
Age	59.1 (9.89)		41–84
Gender			
Female		15 (58)	
Male		11 (42)	
Tumor location			
Frontal		26 (37.1)	
Temporal		14 (20)	
Cerebellum		12 (17.2)	
Parietal		8 (11.4)	
Occipital		6 (8.6)	
Basal ganglia		4 (5.7)	
Tumor localization			
Central		30 (42.9)	
Peripheral		40 (57.1)	
Isocenter distance, mm	59.3 (16.13)		19.8–83
Target volume, cm^3	1.9 (3.14)		0.01–12.4
Euclidian distance between tumor centers, mm	0.6 (0.43)		0.1–2.87
MacDonald longest diameter difference, mm	0.30 (0.297)		0–1.4
MacDonald longest perpendicular diameter difference, mm	0.48 (0.457)		0–2.2
Intersection area	1.9 (3.03)		0.01–12.3
Dice similarity coefficient	0.88 (0.12)		0.46–1
Uncorrected coverage, %	99.4 (0.58)		98.1–100
Corrected coverage, %	91.9 (11.51)		23.1–99.5
Retained coverage	18 (25.7)		
Tumors not meeting criterion for adequacy in SRS plan	52 (74.3)		

SD: Standard deviation.

and GKRS was first employed in treating multiple METs in 1993 (Kihlstrom et al., 1993). These devices utilize multiple ^{60}Co sources to deliver focused radiation to intracranial targets. While GKRS is robust, patient safety requires individual quality assurance measures (Petti et al., 2021). Procedural errors, including imaging-related issues, can contribute to irradiation errors (Derreumaux et al., 2008; Karaiskos et al., 2014; Huq et al., 2016). As GKRS treatment plans predominantly rely on MR imaging, assessing the level of distortion in these images becomes crucial (Grishchuk et al., 2023). Typically, the distortions observed in the image dataset are nonlinear and unevenly distributed, particularly at the periphery of the brain (cortical surface of the brain) and near air-bone interfaces (frontopolar and orbitofrontal cortex, cranial aspects of the prefrontal cortex and the lateral and inferior portions of the temporal lobes), and can be reduced with appropriate MR scanner settings (Wang et al., 2013; Putz et al., 2020). However, diagnostic radiologists may not fully grasp the implications of distortion-related imaging errors in SRS planning.

4.1. Sequence-independent gradient nonlinearity-related distortions

Significant MRI distortions primarily stem from sequence-independent gradient nonlinearity, especially at the periphery of the brain, resulting in shifts of several millimeters (Torfeh et al., 2016). However, these distortions can be corrected using vendor-specific distortion correction methods as a postprocessing step (Baldwin et al., 2007). It is important to highlight that vendor-specific 3D correction should be considered the minimum requirement for SRS planning

(Paulson et al., 2016). While 2D correction is commonly used, it may not be sufficient to prevent substantial shifts in SRS targets (Baldwin et al., 2007; Torfeh et al., 2016). In a study conducted by Seibert et al., (2016), the findings revealed a median displacement of 1.2 mm and a maximum displacement of 3.9 mm in uncorrected images, leading to geographic misses in 28.6% of lesions. Similarly, our study detected a median and maximum displacement of 0.55 and 2.87 mm, respectively. Jacobson et al., (2021) stated that 53% of the targets demonstrated reduced target volume coverage below 98% post-shot correction. In our study, only 25.7% of targets retained 98–100% coverage after correction.

4.2. Sequence-dependent distortions

Another type of distortion relevant to MRI-based intracranial SRS is caused by inhomogeneities in the main magnetic field (B0). These inhomogeneities can arise from residual imperfections in the main magnet as well as magnetic susceptibility effects caused by the patient and necessitate additional correction methods beyond vendor-specific distortion correction (Fransson et al., 2001). A previous GKRS study demonstrated that uncorrected distortion resulting from B0 field inhomogeneities could result in underdosing of tumors (Karaiskos et al., 2014). The impact of B0 inhomogeneities varies with sequence settings and is more pronounced at higher field strengths, such as 3T (Zhang et al., 2010). In our study, although the mean DICE coefficient was slightly lower (0.85 vs. 0.90) for METs scanned with 3T, this difference did not reach statistical significance (p = 0.063). This might be explained by the fact that increasing field strength also increases the signal-to-noise ratio, allowing for higher compensatory readout bandwidths, thus mitigating B0 inhomogeneities (Paulson et al., 2016; Garcia et al., 2018). Furthermore, modern 3T scanners typically possess better shimming capabilities to reduce B0 inhomogeneities compared to many older 1.5T scanners.

Patient-induced perturbations of the B0 field are prominent at air-bone interfaces, particularly near the paranasal sinuses and mastoid cells (Stanescu et al., 2012; Putz et al., 2020). Susceptibility-related distortions in T1-MPRAGE sequences have shown average displacements across the imaged volume of less than 0.5 mm in most cases, but up to 1.6 mm at air-bone boundaries of the sinuses (Wang et al., 2013). We only had three METs at air-bone boundaries, and we did not detect higher distortion in these lesions, probably due to the small number of lesions and the larger tumor volumes (4.57 vs. 1.79 cm^3).

4.3. Distortion correction

Accurate treatment planning in intracranial SRS relies on utilizing appropriate MR images with limited distortions. Consensus guidelines recommend keeping overall distortions below 1 mm, which can be achieved through vendor-specific 3D distortion correction techniques, patient-specific active shimming, and optimized readout bandwidths during MRI acquisition (Paulson et al., 2016). While these measures can significantly reduce distortions, it is important to acknowledge the possibility of residual distortion and potential changes in gradient field properties over time. Theocharis et al., (2022) conducted a study and reported that although geometric accuracy was improved through mean image distortion correction, there remained a residual median distortion of 0.51 mm, which cannot be considered negligible. Therefore, a phantom-based quality assurance program alone may not provide superior geometric accuracy compared to prospective distortion correction in individual patient images. Users should verify whether their stereotactic software has the capability to detect and correct MRI distortion, as not all commercial platforms may have these capabilities (Lightstone et al., 2005). Choosing software that explicitly addresses distortion correction is crucial for accurate treatment planning in intracranial SRS. In our clinical practice, we utilize commercially available Distortion Correction software in addition to vendor-specific correction methods. This software has successfully reduced distortion,
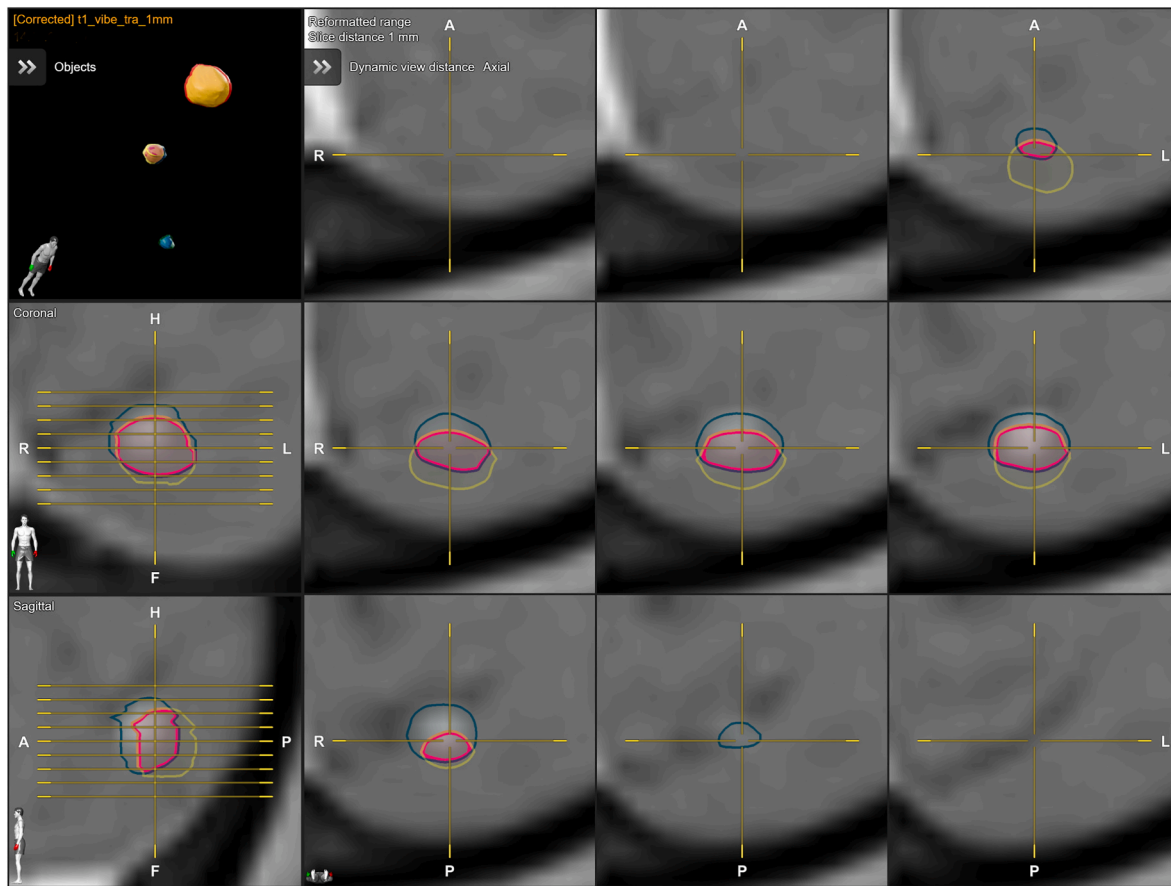
Fig. 3. Corrected tumor volume is outlined in green, and uncorrected tumor volume is outlined in yellow. The displacement of the center of mass is 1.4 mm and the Dice similarity coefficient is 0.57. (For interpretation of the references to colour in this figure legend, the reader is referred to the Web version of this article.)
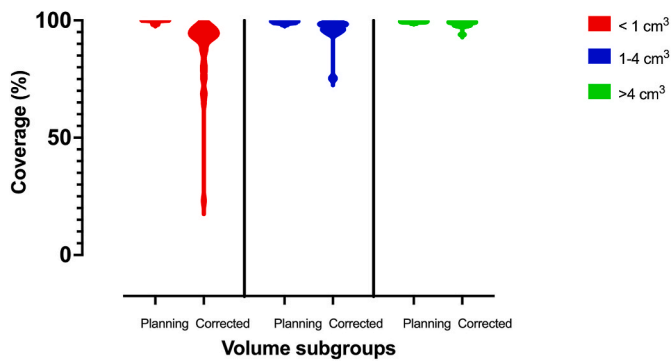

Fig. 4. Violin-plot showing planning and corrected coverage according to volume subgroups.

even in highly distorted images, ensuring accurate image reconstruction and reliable results for SRS treatment planning. Validation studies have shown the effectiveness of the software in reducing distortion and meeting the required accuracy levels (Calvo-Ortega et al., 2019; Retif et al., 2022). Using LGK Icon™ with an integrated CBCT system further enhances workflow flexibility and eliminates distortion caused by the headframe during pre-planning imaging (Petti et al., 2021). This method is rational as using the Leksell GammaPlan treatment-planning software for CT-MR co-registration has been reported to have minor uncertainties, typically measuring 0.3 mm or less (Elekta Instruments, 2015).

In the radiosurgical treatment of METs, treatment planning typically involves adding a margin of 0–2 mm to the gross tumor volume based on immobilization and technology used (Ladbury et al., 2024). Increasing the treatment margin can compensate for distortion in treatment planning; however, it results in larger planning target volumes and larger irradiated volumes of healthy brain tissue (Agazaryan et al., 2021). Predicting the appropriate margin to compensate for distortion is also challenging due to the variability in distortion magnitude across different cases. Research investigating target volume and margin growth calculation using different treatment planning systems has shown significant variations in volume calculations, with differences of up to 10% (Eaton and Alty, 2017). Even when adding margins of the same nominal size to small structures, resulting total volumes can differ by as much as 40%, leading to inconsistent outcomes, especially when treating multiple lesions close together (Grishchuk et al., 2023). For GKRS, patient immobilization with the Leksell Frame and the precise patient positioning system ensures target accuracy and makes additional margins redundant (Skourou et al., 2021; Kutuk et al., 2022). The risk of missing a target due to distortion is primarily influenced by displacement rather than target size. Smaller tumors near the magnet isocenter experience minimal distortion and have a low risk of geometric miss. Larger tumors extending toward the brain's periphery are more susceptible to significant displacement. In a study conducted by Seibert et al., (2016), targets with more than 10% of the volume underdosed were generally smaller, with a median volume of 213 mm^3 compared to the overall median volume of 996 mm^3 across all patients. Similarly, in our study, the underdosed METs were smaller than the rest of the lesions (0.64 cm^3 vs. 1.97 cm^3).

Before proceeding with distortion correction, optimal MRI quality is essential for achieving high accuracy in SRS, which is crucial for successful treatment. However, the emphasis often falls on the technological aspects of treatment delivery, overshadowing the importance of

some recommended practical measures to mitigate potential inaccuracies both in MRI and treatment precision (Putz et al. 2020, 2024; Ladbury et al., 2024). Acquiring an MRI in the treatment position can reduce errors from nonrigid tissue deformation, lower image registration uncertainties, and minimize motion artifacts. This is especially relevant for targets in the medulla oblongata, caudal pons, or cerebellar vermis, where patient positioning differences can affect the accurate targeting due to varied angles of extension influenced by the occipito-atlanto-axial joint complex leading to bending of the brainstem and minor shifts in the location of infratentorial structures (Schmidt and Payne, 2015). It is also crucial to position the patient so that the central region of the target area aligns closely with the magnet's and gradient's isocenter. Another aspect is that the effectiveness of contrast agents in T1 MR sequences for lesion delineation depends on the dose and timing after administration (Yuh et al., 1995). Early imaging (<5 min) might miss smaller lesions, which become more detectable and appear larger at later times or with increased contrast agent doses (Kushnirsky et al., 2016). Administering a double dose of contrast might be considered for enhanced tumor visibility, weighing the benefits of improved delineation against the potential risks of contrast agents. MRI protocols for target delineation should also incorporate at least one 3D sequence, ensuring it has a high enough signal-to-noise ratio to accurately identify treatment targets. The timing between MRI and treatment is also critical for accuracy in SRS. Studies have shown that longer intervals between imaging and treatment can significantly affect local control rates and may necessitate changes in treatment planning (Seymour et al., 2015). In our practice, we use same-day imaging; however, in case of a contraindication to repeat MRI, we have set a strict guideline that the time between MRI images and SRS should not surpass two days.

Besides being validated to be a useful supplementary tool after optimal prior knowledge-based distortion correction, registration-based distortion correction, as used in Elements Cranial Distortion Correction (Brainlab AG, Munich, Germany), faces significant limitations: (1) the accuracy of the non-rigid registration declines as the deformation between image datasets increases, and (2) unlike methods that utilize prior knowledge, it does not consistently enhance the geometric accuracy of corrected images across all clinical scenarios. This is due to potential local convergence of iterative algorithms or insufficient constraints in cases where the CT images lack clear differentiation between targets and surrounding tissue (Putz et al., 2024).

4.4. Limitations

This study has limitations, including its reliance on a sample from a single institution, which limits generalizability to the broader population. However, the observed degree of distortion aligns with previous research (Moerland et al., 1995; Stanescu et al., 2008; Seibert et al., 2016). It is important to note that the study focused solely on intracranial SRS planning and emphasized the significance of distortion in this context, as correction for distortion effects is not widely implemented in clinical practice. Nonetheless, the findings clearly indicate that MR distortion can significantly affect the accuracy of SRS planning. Although a comprehensive comparison with all available software solutions was beyond the scope of our study, follow-up studies focusing on comparing different distortion correction methodologies and their impact on SRS planning accuracy could be useful.

5. Conclusions

Incorporating distortion correction as a standard procedure for precise SRS planning is crucial. Each center should evaluate its own workflow and engage in discussions with radiology departments, if applicable, to guarantee the anatomical accuracy of MRI for SRS. Referring patients at risk of significant distortion to centers employing distortion correction is another option to consider.

References

Agazaryan, N., Tenn, S., Lee, C., Steinberg, M., Hegde, J., Chin, R., et al., 2021. Simultaneous radiosurgery for multiple brain metastases: technical overview of the UCLA experience. Radiat. Oncol. 16 (1), 221. https://doi.org/10.1186/s13014-021-01944-w.

Baldwin, L.N., Wachowicz, K., Thomas, S.D., Rivest, R., Fallone, B.G., 2007. Characterization, prediction, and correction of geometric distortion in 3 T MR images. Med. Phys. 34 (2), 388–399. https://doi.org/10.1118/1.2402331.

Benjamin, C.G., Gurewitz, J., Kavi, A., Bernstein, K., Silverman, J., Mureb, M., et al., 2021. Survival and outcomes in patients with $>/=$ 25 cumulative brain metastases treated with stereotactic radiosurgery. J. Neurosurg. 1–11. https://doi.org/10.3171/2021.9.JNS21882.

Bowden, G., Faramand, A., Niranjan, A., Lunsford, L.D., Monaco 3rd, E., 2019. Gamma knife radiosurgery for the management of more than 15 cerebral metastases. World Neurosurg. 126, e989–e997. https://doi.org/10.1016/j.wneu.2019.03.019.

Brock, K.K., Mutic, S., McNutt, T.R., Li, H., Kessler, M.L., 2017. Use of image registration and fusion algorithms and techniques in radiotherapy: report of the AAPM radiation therapy Committee task group No. 132. Med. Phys. 44 (7), e43–e76. https://doi.org/10.1002/mp.12256.

Calvo-Ortega, J.F., Mateos, J., Alberich, A., Moragues, S., Acebes, J.J., Jose, S.S., Casals, J., 2019. Evaluation of a novel software application for magnetic resonance distortion correction in cranial stereotactic radiosurgery. Med. Dosim. 44 (2), 136–143. https://doi.org/10.1016/j.meddos.2018.04.002.

Chang, H., Fitzpatrick, J.M., 1992. A technique for accurate magnetic resonance imaging in the presence of field inhomogeneities. IEEE Trans. Med. Imag. 11 (3), 319–329. https://doi.org/10.1109/42.158935.

Derreumaux, S., Etard, C., Huet, C., Trompier, F., Clairand, I., Bottollier-Depois, J.F., et al., 2008. Lessons from recent accidents in radiation therapy in France. Radiat. Protect. Dosim. 131 (1), 130–135. https://doi.org/10.1093/rpd/ncn235.

Dice, L.R., 1945. Measures of the amount of ecologic association between species. Ecology 26 (3), 297–302. https://doi.org/10.2307/1932409.

Eaton, D.J., Alty, K., 2017. Dependence of volume calculation and margin growth accuracy on treatment planning systems for stereotactic radiosurgery. Br. J. Radiol. 90 (1080), 20170633 https://doi.org/10.1259/bjr.20170633.

Elekta Instruments, A.B., 2015. Accuracy of co-registration of planning images with Cone Beam CT images. from. https://www.elekta.com/medical-affairs/bibliographies/Accuracy%20of%20co-registration%20of%20planning%20images%20with%20Cone%20Beam%20CT%20images%20white%20paper.pdf.

Fransson, A., Andreo, P., Potter, R., 2001. Aspects of MR image distortions in radiotherapy treatment planning. Strahlenther. Onkol. 177 (2), 59–73. https://doi.org/10.1007/pl00002385.

Garcia, M.A., Anwar, M., Yu, Y., Duriseti, S., Merritt, B., Nakamura, J., et al., 2018. Brain metastasis growth on preradiosurgical magnetic resonance imaging. Pract. Radiat. Oncol. 8 (6), e369–e376. https://doi.org/10.1016/j.prro.2018.06.004.

Grishchuk, D., Dimitriadis, A., Sahgal, A., De Salles, A., Fariselli, L., Kotecha, R., et al., 2023. ISRS technical guidelines for stereotactic radiosurgery: treatment of small brain metastases (</=1 cm in diameter). Pract. Radiat. Oncol. 13 (3), 183–194. https://doi.org/10.1016/j.prro.2022.10.013.

Hiepe, P., 2017. Cranial Distortion Correction - Technical Background, vol. 2023 from. https://www.researchgate.net/publication/317359164_Cranial_Distortion_Correction_-_Technical_Background.

Huq, M.S., Fraass, B.A., Dunscombe, P.B., Gibbons Jr., J.P., Ibbott, G.S., Mundt, A.J., et al., 2016. The report of Task Group 100 of the AAPM: application of risk analysis methods to radiation therapy quality management. Med. Phys. 43 (7), 4209. https://doi.org/10.1118/1.4947547.

Jacobson, S., Jones, C., Lusk, R., Jenkins, M., Chamunyonga, C., Pinkham, M.B., Brown, E., 2021. Clinical impact of magnetic resonance imaging distortions on gamma knife radiosurgery. J. Med. Radiat. Sci. 68 (3), 274–281. https://doi.org/10.1002/jmrs.472.

Jezzard, P., Balaban, R.S., 1995. Correction for geometric distortion in echo planar images from B0 field variations. Magn. Reson. Med. 34 (1), 65–73. https://doi.org/10.1002/mrm.1910340111.

Karaiskos, P., Moutsatsos, A., Pappas, E., Georgiou, E., Roussakis, A., Torrens, M., Seimenis, I., 2014. A simple and efficient methodology to improve geometric accuracy in gamma knife radiation surgery: implementation in multiple brain metastases. Int. J. Radiat. Oncol. Biol. Phys. 90 (5), 1234–1241. https://doi.org/10.1016/j.ijrobp.2014.08.349.

Kihlstrom, L., Karlsson, B., Lindquist, C., 1993. Gamma Knife surgery for cerebral metastases. Implications for survival based on 16 years experience. Stereotact. Funct. Neurosurg. 61 (Suppl. 1), 45–50. https://doi.org/10.1159/000100659.

Kushnirsky, M., Nguyen, V., Katz, J.S., Steinklein, J., Rosen, L., Warshall, C., et al., 2016. Time-delayed contrast-enhanced MRI improves detection of brain metastases and apparent treatment volumes. J. Neurosurg. 124 (2), 489–495. https://doi.org/10.3171/2015.2.JNS141993.

Kutuk, T., Kotecha, R., Tolakanahalli, R., Wieczorek, D.J.J., Lee, Y.C., Ahluwalia, M.S., et al., 2022. Zero setup margin mask versus frame immobilization during gamma knife((R)) Icon stereotactic radiosurgery for brain metastases. Cancers 14 (14). https://doi.org/10.3390/cancers14143392.

Ladbury, C., Pennock, M., Yilmaz, T., Ankrah, N.K., Andraos, T., Gogineni, E., et al., 2024. Stereotactic radiosurgery in the management of brain metastases: a case-based radiosurgery society practice guideline. Adv. Radiat. Oncol. 9 (3), 101402 https://doi.org/10.1016/j.adro.2023.101402.

Leksell, L., 1951. The stereotaxic method and radiosurgery of the brain. Acta Chir. Scand. 102 (4), 316–319.

Lightstone, A.W., Benedict, S.H., Bova, F.J., Solberg, T.D., Stern, R.L., 2005a. Intracranial stereotactic positioning systems: report of the American association of physicists in medicine radiation therapy committee task group No. 68. Med. Phys. 32 (7Part1), 2380–2398. https://doi.org/10.1118/1.1945347.

Lightstone, A.W., Benedict, S.H., Bova, F.J., Solberg, T.D., Stern, R.L., C. American Association of Physicists in Medicine Radiation Therapy, 2005b. Intracranial stereotactic positioning systems: report of the American association of physicists in medicine radiation therapy committee task group no. 68. Med. Phys. 32 (7), 2380–2398. https://doi.org/10.1118/1.1945347.

Macdonald, D.R., Cascino, T.L., Schold Jr., S.C., Cairncross, J.G., 1990. Response criteria for phase II studies of supratentorial malignant glioma. J. Clin. Oncol. 8 (7), 1277–1280. https://doi.org/10.1200/JCO.1990.8.7.1277.

Moerland, M.A., Beersma, R., Bhagwandien, R., Wijrdeman, H.K., Bakker, C.J., 1995. Analysis and correction of geometric distortions in 1.5 T magnetic resonance images for use in radiotherapy treatment planning. Phys. Med. Biol. 40 (10), 1651–1654. https://doi.org/10.1088/0031-9155/40/10/007.

Morgan, P.S., Bowtell, R.W., McIntyre, D.J., Worthington, B.S., 2004. Correction of spatial distortion in EPI due to inhomogeneous static magnetic fields using the reversed gradient method. J. Magn. Reson. Imag. 19 (4), 499–507. https://doi.org/10.1002/jmri.20032.

Niranjan, A., Monaco, E., Flickinger, J., Lunsford, L.D., 2019. Guidelines for multiple brain metastases radiosurgery. Prog. Neurol. Surg. 34, 100–109. https://doi.org/10.1159/000493055.

Pappas, E.P., Alshanqity, M., Moutsatsos, A., Lababidi, H., Alsafi, K., Georgiou, K., et al., 2017. MRI-related geometric distortions in stereotactic radiotherapy treatment planning: evaluation and dosimetric impact. Technol. Cancer Res. Treat. 16 (6), 1120–1129. https://doi.org/10.1177/1533034617735454.

Pappas, E.P., Seimenis, I., Moutsatsos, A., Georgiou, E., Nomikos, P., Karaiskos, P., 2016. Characterization of system-related geometric distortions in MR images employed in Gamma Knife radiosurgery applications. Phys. Med. Biol. 61 (19), 6993–7011. https://doi.org/10.1088/0031-9155/61/19/6993.

Paulson, E.S., Crijns, S.P., Keller, B.M., Wang, J., Schmidt, M.A., Coutts, G., van der Heide, U.A., 2016. Consensus opinion on MRI simulation for external beam radiation treatment planning. Radiother. Oncol. 121 (2), 187–192. https://doi.org/10.1016/j.radonc.2016.09.018.

Petti, P.L., Rivard, M.J., Alvarez, P.E., Bednarz, G., Daniel Bourland, J., DeWerd, L.A., et al., 2021. Recommendations on the practice of calibration, dosimetry, and quality assurance for gamma stereotactic radiosurgery: report of AAPM Task Group 178. Med. Phys. 48 (7), e733–e770. https://doi.org/10.1002/mp.14831.

Putz, F., Bock, M., Schmitt, D., Bert, C., Blanck, O., Ruge, M.I., et al., 2024. Quality requirements for MRI simulation in cranial stereotactic radiotherapy: a guideline from the German Taskforce "Imaging in Stereotactic Radiotherapy". Strahlenther. Onkol. 200 (1), 1–18. https://doi.org/10.1007/s00066-023-02183-6.

Putz, F., Mengling, V., Perrin, R., Masitho, S., Weissmann, T., Rosch, J., et al., 2020. Magnetic resonance imaging for brain stereotactic radiotherapy : a review of requirements and pitfalls. Strahlenther. Onkol. 196 (5), 444–456. https://doi.org/10.1007/s00066-020-01604-0.

Retif, P., Djibo Sidikou, A., Mathis, C., Letellier, R., Verrecchia-Ramos, E., Dupres, R., Michel, X., 2022. Evaluation of the ability of the Brainlab Elements Cranial Distortion Correction algorithm to correct clinically relevant MRI distortions for cranial SRT. Strahlenther. Onkol. 198 (10), 907–918. https://doi.org/10.1007/s00066-022-01988-1.

Samanci, Y., Sisman, U., Altintas, A., Sarioglu, S., Sharifi, S., Atasoy, A.I., et al., 2021. Hypofractionated frameless gamma knife radiosurgery for large metastatic brain tumors. Clin. Exp. Metastasis 38 (1), 31–46. https://doi.org/10.1007/s10585-020-10068-6.

Schmidt, M.A., Payne, G.S., 2015. Radiotherapy planning using MRI. Phys. Med. Biol. 60 (22), R323–R361. https://doi.org/10.1088/0031-9155/60/22/R323.

Seibert, T.M., White, N.S., Kim, G.Y., Moiseenko, V., McDonald, C.R., Farid, N., et al., 2016. Distortion inherent to magnetic resonance imaging can lead to geometric miss in radiosurgery planning. Pract. Radiat. Oncol. 6 (6), e319–e328. https://doi.org/10.1016/j.prro.2016.05.008.

Seymour, Z.A., Fogh, S.E., Westcott, S.K., Braunstein, S., Larson, D.A., Barani, I.J., et al., 2015. Interval from imaging to treatment delivery in the radiation surgery age: how long is too long? Int. J. Radiat. Oncol. Biol. Phys. 93 (1), 126–132. https://doi.org/10.1016/j.ijrobp.2015.05.001.

Skourou, C., Hickey, D., Rock, L., Houston, P., Sturt, P., O'Sullivan, S., et al., 2021. Treatment of multiple intracranial metastases in radiation oncology: a contemporary review of available technologies. BJR Open 3 (1), 20210035. https://doi.org/10.1259/bjro.20210035.

Stanescu, T., Jans, H.S., Pervez, N., Stavrev, P., Fallone, B.G., 2008. A study on the magnetic resonance imaging (MRI)-based radiation treatment planning of intracranial lesions. Phys. Med. Biol. 53 (13), 3579–3593. https://doi.org/10.1088/0031-9155/53/13/013.

Stanescu, T., Wachowicz, K., Jaffray, D.A., 2012. Characterization of tissue magnetic susceptibility-induced distortions for MRIgRT. Med. Phys. 39 (12), 7185–7193. https://doi.org/10.1118/1.4764481.

Stanley, J., Dunscombe, P., Lau, H., Burns, P., Lim, G., Liu, H.W., et al., 2013. The effect of contouring variability on dosimetric parameters for brain metastases treated with stereotactic radiosurgery. Int. J. Radiat. Oncol. Biol. Phys. 87 (5), 924–931. https://doi.org/10.1016/j.ijrobp.2013.09.013.

Theocharis, S., Pappas, E.P., Seimenis, I., Kouris, P., Dellios, D., Kollias, G., Karaiskos, P., 2022. Geometric distortion assessment in 3T MR images used for treatment planning in cranial Stereotactic Radiosurgery and Radiotherapy. PLoS One 17 (5), e0268925. https://doi.org/10.1371/journal.pone.0268925.

Torfeh, T., Hammoud, R., Perkins, G., McGarry, M., Aouadi, S., Celik, A., et al., 2016. Characterization of 3D geometric distortion of magnetic resonance imaging scanners commissioned for radiation therapy planning. Magn. Reson. Imaging 34 (5), 645–653. https://doi.org/10.1016/j.mri.2016.01.001.

Vogelbaum, M.A., Brown, P.D., Messersmith, H., Brastianos, P.K., Burri, S., Cahill, D., et al., 2022. Treatment for brain metastases: ASCO-SNO-ASTRO guideline. J. Clin. Oncol. 40 (5), 492–516. https://doi.org/10.1200/JCO.21.02314.

Walker, A., Liney, G., Metcalfe, P., Holloway, L., 2014. MRI distortion: considerations for MRI based radiotherapy treatment planning. Australas. Phys. Eng. Sci. Med. 37 (1), 103–113. https://doi.org/10.1007/s13246-014-0252-2.

Wang, D., Strugnell, W., Cowin, G., Doddrell, D.M., Slaughter, R., 2004. Geometric distortion in clinical MRI systems Part I: evaluation using a 3D phantom. Magn. Reson. Imaging 22 (9), 1211–1221. https://doi.org/10.1016/j.mri.2004.08.012.

Wang, H., Balter, J., Cao, Y., 2013. Patient-induced susceptibility effect on geometric distortion of clinical brain MRI for radiation treatment planning on a 3T scanner. Phys. Med. Biol. 58 (3), 465–477. https://doi.org/10.1088/0031-9155/58/3/465.

Wei, Z., Niranjan, A., Abou-Al-Shaar, H., Deng, H., Albano, L., Lunsford, L.D., 2022. A volume matched comparison of survival after radiosurgery in non-small cell lung cancer patients with one versus more than twenty brain metastases. J. Neuro Oncol. 157 (3), 417–423. https://doi.org/10.1007/s11060-022-03981-1.

Weygand, J., Fuller, C.D., Ibbott, G.S., Mohamed, A.S., Ding, Y., Yang, J., et al., 2016. Spatial precision in magnetic resonance imaging-guided radiation therapy: the role of geometric distortion. Int. J. Radiat. Oncol. Biol. Phys. 95 (4), 1304–1316. https://doi.org/10.1016/j.ijrobp.2016.02.059.

Yamamoto, M., Serizawa, T., Sato, Y., Higuchi, Y., Kasuya, H., 2021. Stereotactic radiosurgery results for patients with 5-10 versus 11-20 brain metastases: a retrospective cohort study combining 2 databases totaling 2319 patients. World Neurosurg. 146, e479–e491. https://doi.org/10.1016/j.wneu.2020.10.124.

Yuh, W.T., Tali, E.T., Nguyen, H.D., Simonson, T.M., Mayr, N.A., Fisher, D.J., 1995. The effect of contrast dose, imaging time, and lesion size in the MR detection of intracerebral metastasis. AJNR Am. J. Neuroradiol. 16 (2), 373–380.

Zhang, B., MacFadden, D., Damyanovich, A.Z., Rieker, M., Stainsby, J., Bernstein, M., et al., 2010. Development of a geometrically accurate imaging protocol at 3 Tesla MRI for stereotactic radiosurgery treatment planning. Phys. Med. Biol. 55 (22), 6601–6615. https://doi.org/10.1088/0031-9155/55/22/002.